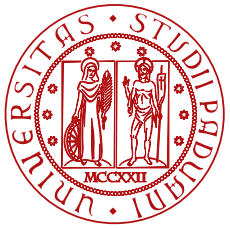

Università degli Studi di Padova

NTNU

Department of Engineering Cybernetics

Master Thesis in Control Systems Engineering

Data-Driven Control-oriented Modelling of Submerged Arc Furnaces

Master Candidate

Pierangelo Fornasier

Student ID 2027911

Supervisor

Damiano Varagnolo

Norwegian University of Science and Technology

Academic Year
2022/2023

Abstract

The present thesis focuses on the integration of chemophysical knowledge and data-driven insights to develop control-oriented models for submerged arc furnaces (SAF). The primary objective of this research is to facilitate the metallurgical processes involved in the production of ferrosilicon (FeSi).

The state-of-art of simulators utilized for submerged arc furnaces is founded upon a static meta-model, that functions as a data-driven substitute for Physic-based Finite Element Methods (FEM) models.

The aim of this study is to develop a linear dynamic model utilizing data-driven techniques from the system identification literature, and subsequently try to evaluate its performance in comparison to the meta-model. The current thesis addresses the difficulties associated with this specific task and suggests potential solutions for overcoming them.

Sommario

La tesi si concentra sull'integrazione delle conoscenze chimico-fisiche in un approccio data-driven per sviluppare dei modelli orientati al controllo di fornaci ad arco sommerso (SAF). L'obiettivo primario di questa ricerca è quello di facilitare la comprensione dei processi metallurgici coinvolti nella produzione di ferrosilicio (FeSi).

Lo stato dell'arte dei simulatori utilizzati per le fornaci ad arco sommerso è basato su un meta-modello statico, derivato a sua volta da un modello basato sul metodo degli elementi finiti (FEM).

L'obiettivo di questo studio è sviluppare un modello dinamico e lineare che utilizzi le tecniche di identificatione dei sistemi (systems identification) e di valutare le sue prestazioni rispetto al meta-modello. La tesi approfondisce le difficoltà associate a questo obiettivo e suggerisce potenziali soluzioni per superarle.

Contents

List of Figures

1 Introduction

The production of ferrosilicon alloys in three-phase electric submerged-arc furnaces consumes large amounts of electric energy. The control of a ferrosilicon furnace has proven to be intricate due to its complex nature, which involves multiple interrelated sub-processes encompassing metallurgical (chemical), thermal, electrical, and mechanical processes. However, as a ferrosilicon furnace is a complex process consisting of various closely interacting sub-processes, such as metallurgical (chemical), thermal, electrical and mechanical processes, the control of such a furnace has turned out to be quite complicated.

The main problems are the lack of direct measurements of the process variables in the heart of the furnace, as well as the limited understanding of the intricate interplay among the electrical, thermal, and metallurgical conditions within the furnace [1].

The thesis provides a broad overview of the operational principles underlying a submerged arc furnace. It also discusses the procedure for acquiring a linear data-driven model and draws a comparison between this approach and an existing metamodel.

The thesis is written for the research institute NORCE and the analyses are part of their project *Electrical Conditions in Submerged Arc Furnaces – Identification and Improvement (SAFECI)*. The project spans from 2021 to 2025 and is funded by The Research Council of Norway and the industrial partners Elkem, Eramet Norway, Finnfjord and Wacker Chemicals Norway. NTNU also contributes as a research partner.

2

Submerged Arc Furnaces

2.1 Submerged Arc Furnaces

The data utilized in this study was obtained from a Submerged Arc Furnace belonging to Wacker Chemicals, a prominent metal manufacturer in Norway. The Furnace generates Ferrosilicon (FeSi), a chemical compound comprising 75% silicon and 25% iron. The manufacturing of this substance, commonly accomplished via a metallurgical methodology, holds substantial practical and economic importance [2].

An illustration of the Submerged Arc Furnace (SAF) is given in figure 2.1 [3].

The geometry of SAF can be described as cylindrical. Raw materials, including quartz and coal, are combined and introduced into the furnace from its uppermost point.

The picture depicted in Figure 2.1 illustrates the process by which energy is supplied to three electrodes via a transformer, subsequently leading to the flow of electrical currents into the molten material that will ultimately result in the formation of FeSi. Ideally, the currents generated by the electrodes should be directed towards the lowermost part of the furnace. The aforementioned zone encompasses not only the electrodes, but also a heated sub-zone, typically situated beneath said electrodes, which harbors the majority of the electrical resistance.

The burden zone is a stratum of melted substance located above the lower layer, which encompasses the constituents required for the aimed chemical reaction. The region known as the hot zone exhibits a notable level of resistance. The passage of electrical currents through the substance results in the produc-

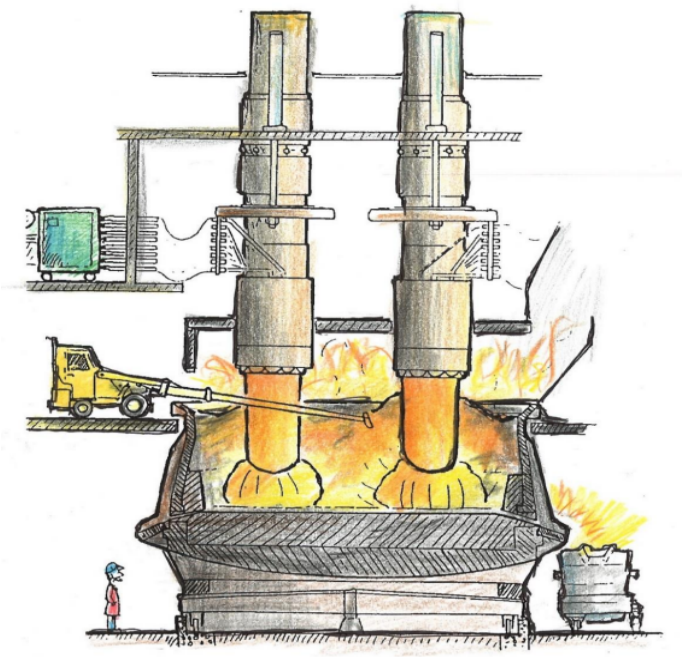

Figure 2.1: Illustration of a furnace.

tion of a considerable quantity of thermal energy, thereby promoting the chemical reaction and facilitating the creation of FeSi (FerroSilicon).

2.1.1 Electrodes

The furnace is equipped with three Söderberg electrodes [4] that are arranged in an equilateral triangle configuration and are fully immersed in the raw materials [3].

The electrodes hold an electrical charge. The induction of an arc within the furnace generates elevated temperatures, thereby facilitating a series of chemical reactions [3].

The vertical movements of the electrodes are constrained by their physical limitations. The vertical displacement range of the electrode holders is 120 cm.

Given that the electrodes are depleted during furnace operation, a distinct control mechanism is implemented to manage electrode replenishment. This process, referred to as electrode slipping, serves to offset the electrode consumption that occurs during operation. Over an extended duration, the amount of slipping must be commensurate with the overall consumption of electrodes [5].

The rate of slipping is modulated in response to the holder position's prede-

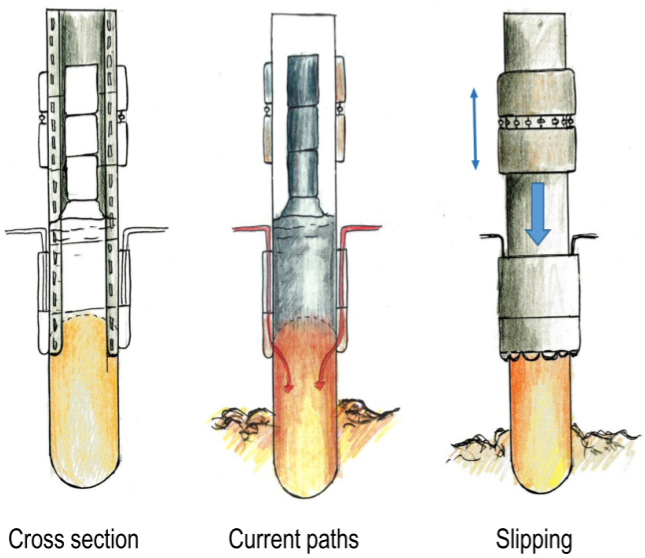

Figure 2.2: Söderberg electrodes

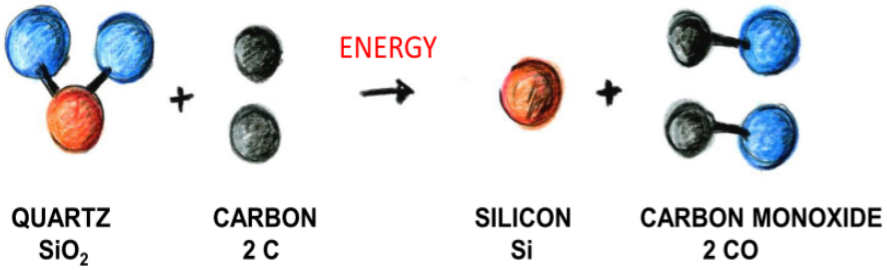

Figure 2.3: Main reaction inside the furnace. Silicon is then mixed with iron.

termined setpoint.The objective is to maintain the position of the holder at the reference point while ensuring that the resistance within the furnace remains unaffected.

The measurement of the tip position of the electrodes is currently unavailable. The rate of slippage and the positioning of the electrodes are established, however, the consumption of the electrodes within the furnace is merely approximated. The determination of the tip location of the electrodes remains a challenge, as the precision of the current estimation does not align with the level of accuracy sought by furnace operators.

The displacement of a single electrode has a consequential impact not only on the electrical current flowing through it, but also on the electrical current flowing through the remaining two electrodes.[6] This implies that there exists

a significant level of interdependence among the measurements associated with distinct electrodes.

2.1.2 FURNACE'S CONTROL SYSTEM

The regulation of the furnace is achieved through the specification of a power setpoint and an electrical resistance setpoint. The furnace has a limited number of control actions, specifically three:

- Adjust the power given by the transformer
- Adjust the position of the electrodes vertically
- Modifying the quantity and composition of the charged material can alter the conductivity within the furnace.

The regulation of resistance is achieved through the vertical displacement of the electrodes. There exist upper and lower limits of resistance. In the event that the measured resistance falls below the predetermined lower threshold, the electrode will be elevated, resulting in an increase in resistance. Conversely, if the resistance exceeds the desired upper limit, the electrode will be lowered to decrease the resistance.

The control system exhibits a partial manual operation, whereby the metallurgists specify the quantity and composition of the charge material, which subsequently affects the electrical conditions within the furnace.

Electrical control is considerably quicker than chemical control. The process of mixing with a new composition typically requires several hours before it reaches the reactive zones and exerts its influence on the process.

2.1.3 SOME NOTES ABOUT THE DISTURBANCES

The measurement systems are susceptible to significant measurement distortions due to the presence of high temperatures and intense magnetic fields resulting from substantial conductance variations in the charge and electrode-to-earth voltages, which adversely impact the sensors. The Böckman principle is utilized to measure the voltage as a partial solution to the problem:

> *Three measuring leads in approximately 120° symmetry are used to reproduce the furnace bottom potential above the furnace, where it is connected to the star point above between the electrode voltages. The idea is that the*

voltages induced in the three measuring leads will compensate each other. Deviation from ideal 120° symmetry which may be necessary for practical reasons is compensated by adjusting a resistor network connecting the three leads [7].

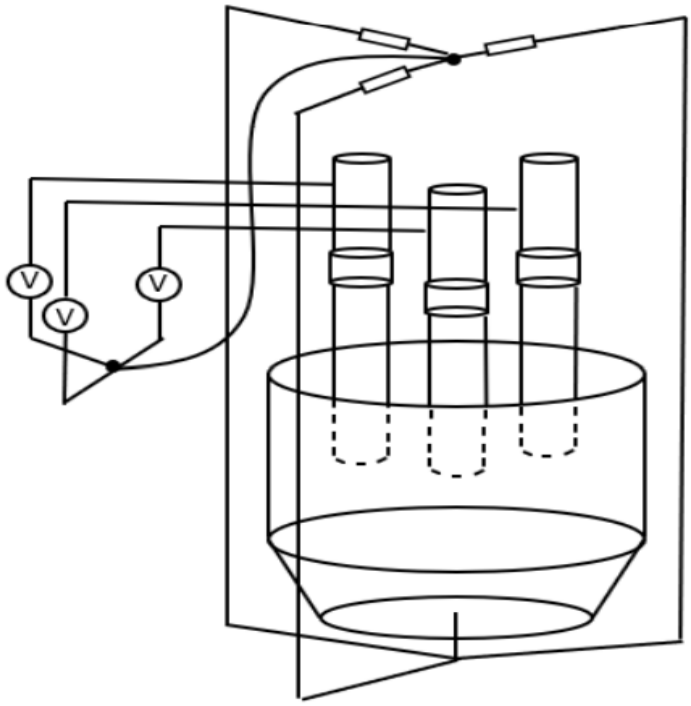

Figure 2.4: Böckman principle. The voltage in the bottom is moved to an area with weak magnetic fields

In addition, it should be noted that a portion of the electrode currents is often redirected in unfavorable pathways, such as between the electrodes, rather than being directed downward towards the furnace base to facilitate the production of heat for chemical reactions [2].

3

Data Preprocessing

3.1 Data imputation

As described in section 2.1.3, the dataset exhibits significant levels of noise as a result of the inherent challenges associated with measuring the system.

Furthermore, the dataset exhibits a significant number of outliers that cannot be disregarded. Outliers are data points that exhibit substantial deviation from the remaining observations. In order to address outliers, they are systematically eliminated and substituted with alternative values that are considered more plausible.

Outliers can be characterized as elements that are situated at a distance greater than three times the scaled median absolute deviation from the median. The scaled median absolute deviation (MAD) is a statistical measure that is formally defined as follows:

$$c * median(|(A - median(A)|) \tag{3.1}$$

where

$$c = \frac{-1}{\sqrt{2} * erfcinv(3/2)} \tag{3.2}$$

and $erfcinv$ is the inverse complementary error function.

Outliers have been classified as missing values and replaced with MICE algorithm.

3.1.1 Multivariate Imputation By Chained Equations

The MICE (Multivariate Imputation by Chained Equations) algorithm employs a statistical approach to estimate the missing values of each feature by modeling it as a function of other features, and subsequently utilizes this estimate for imputation. The process operates in an iterative round-robin manner whereby, during each step, a specific feature column is selected as the output variable y, while the remaining feature columns are considered as input variables X. [8]

A regression model is trained on a dataset consisting of input variables X and known output variable y. Subsequently, the regressor is employed to make predictions for the absent y values. The process is executed iteratively for each feature and is subsequently replicated for multiple imputation rounds. [9]

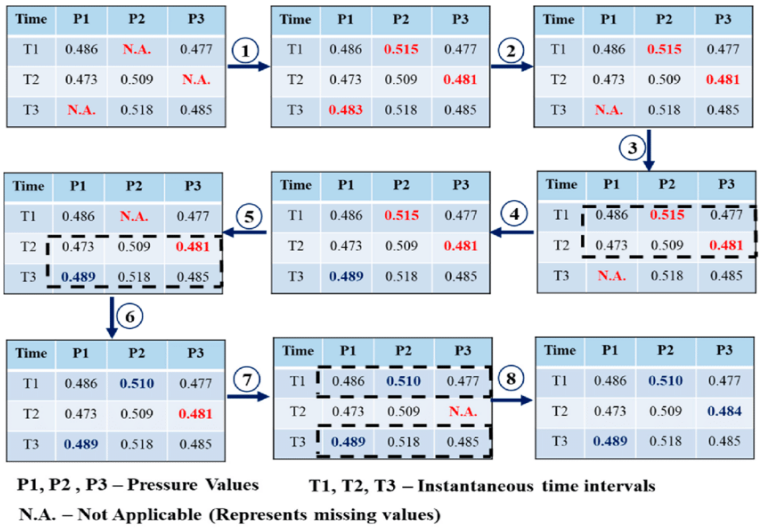

Figure 3.1: Example of MICE algorithm

Figure 3.1 shows 1 imputation round of a 3-by-3 matrix with 3 missing values. The process in question is known to introduce a certain degree of error or noise into the dataset.

The chained equation process can be broken down into four general steps:[10]

Step 1: A simple imputation, such as imputing the mean, is performed for every missing value in the dataset. These mean imputations can be thought of as "place holders."

Step 2: The "place holder" mean imputations for one variable ("var") are set back to missing.

Step 3: The observed values from the variable "var" in Step 2 are regressed on the other variables in the imputation model, which may or may not consist of all of the variables in the dataset. In other words, "var" is the dependent variable in a regression model and all the other variables are independent variables in the regression model. These regression models operate under the same assumptions that one would make when performing linear, logistic, or Poison regression models outside of the context of imputing missing data.

Step 4: The missing values for "var" are then replaced with predictions (imputations) from the regression model. When "var" is subsequently used as an independent variable in the regression models for other variables, both the observed and these imputed values will be used.

Step 5: Steps 2–4 are then repeated for each variable that has missing data. The cycling through each of the variables constitutes one iteration or "cycle." At the end of one cycle all of the missing values have been replaced with predictions from regressions that reflect the relationships observed in the data.

Step 6: Steps 2–4 are repeated for a number of cycles, with the imputations being updated at each cycle.

This thesis has overlooked the errors linked to the adopted methodology.

3.2 Data Normalization

The Euclidean norm, also known as the L-2 norm, has been employed for the purpose of scaling each individual feature. The L-2 norm is a widely used method for scaling features. Values are rescaled to be in the range of 0 and 1.

In comparison with alternative approaches, such as standardization, the L-2 norm preserves the original distribution's shape, making it particularly advantageous in cases where the data distribution deviates from a Gaussian distribution.

$$||V||_2 = \sqrt{\sum_{k=1}^{N} |v_k|^2} \tag{3.3}$$

where N is the number of samples for each feature and v_k represents the k-th sample of the variable.

Normalization also serves the purpose of obscuring the proprietary data.

4 Features Selection

4.1 Output selection

The primary variables that exhibit a strong correlation with the overall production levels are the electrode currents [2].

The current within the electrodes cannot be arbitrarily set by the operator, but it is a valuable parameter for determining how to adjust the voltage and holder position.

The electrode currents have been selected as outputs of the dynamic model due to the aforementioned reasons.

4.2 Features excluded

Several variables in the dataset are computed using established equations that incorporate the output (current) as a parameter. (see appendix A.1).

Parameters removed
Total furnace resistance
Electrode resistances
Furnace C3
Electrode power
Electrode power factor
Electrode reactances

and they have been removed for future analysis.

In the pursuit of comparing the dynamic model to the static meta-model, the dataset pertaining to the electrodes' holder position has been excluded. Additional clarifications will be provided in section (7.3).

4.3 Lasso Regression

The LASSO (Least Absolute Shrinkage and Selection Operator) is a regression analysis technique that combines variable selection and regularisation to improve the predictive accuracy and interpretability of the resulting statistical model.

This strategy was adopted for two reasons:

- The exclusion of irrelevant features that do not contribute to the construction of the dynamic model.
- The use of additional features leads to an increase in the complexity of the model.

Lasso regression is utilised in order to identify the most significant variables for predicting the current.

For a given value of λ, a non-negative parameter, lasso solves the problem:

$$\min_{\beta_0,\beta}\left(\frac{1}{2N}\sum_{i=1}^{N}\left(y_i-\beta_0-x_i^T\beta\right)^2+\lambda\sum_{j=1}^{p}\left|\beta_j\right|\right) \tag{4.1}$$

subject to

$$\sum_{j=1}^{p}\left|\beta_j\right|\leq t \tag{4.2}$$

with:

- $t \geq 0$ is a tuning parameter.
- N is the number of observations.
- y_i is the current at observation i.
- x_i is measurement data,a vector of length p, at observation i.

For a given value of λ, the variables that are associated with a non-zero component of β exhibit greater significance in comparison to the variables that are linked to a zero component of β.

As the value of λ decreases, there is an increase in the quantity of non-zero elements within the vector β.

The Lasso regression method computes the coefficients of the least-squares regression model that provides the optimal fit for a linear model, based on the input data (X) and output data (y) [11].

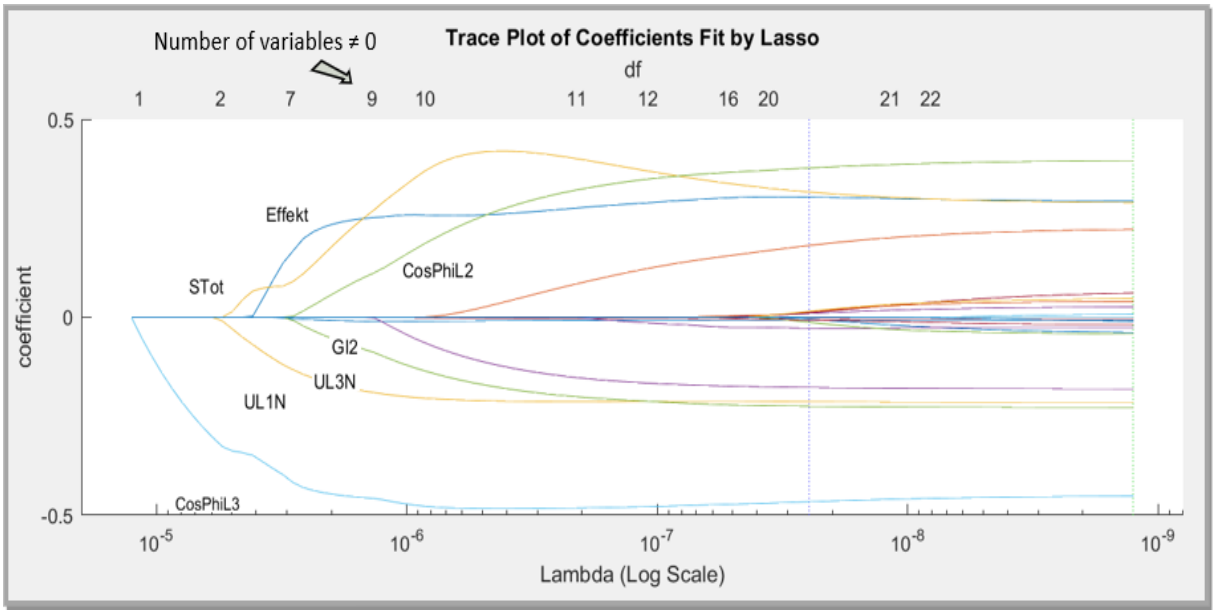

Figure 4.1: Lasso Plot for current of electrode 1

Figure 4.1 displays the logarithmic lasso plot of the current observed in the first electrode. Starting from the leftmost side, it appears evident that only one coefficient displays a non-zero value. This suggests that the variable mentioned above is of great importance in predicting the current.

As Lambda decreases, an increasing number of feature coefficients deviate from zero, ultimately resulting in a scenario where all coefficients on the right-hand side are non-zero. The quantity of non-zero coefficients is indicated in the upper section of figure 4.1.

4.4 Inputs

The Lasso regression technique has been employed thrice, with each application pertaining to a distinct electrode current.

The variables that have been chosen for the dynamic model are:

Table 4.1: Key variables for the prediction of each current

Current 1	**Current 2**	**Current 3**
$cos(\phi_3)$	$cos(\phi_1)$	$cos(\phi_2)$
V_1	$STot$	$STot$
$STot$	V_2	V_2
$P(MW)$	$P(MW)$	$P(MW)$
$cos(\phi_2)$	$cos(\phi_3)$	$cos(\phi_1)$
V_3		V_3

Table 4.1 presents the input variables chosen for the dynamic model corresponding to each electrode current. These features are arranged in a descending order based on their level of significance.

There are a total of eight distinct variables:

1. $P(MW)$ Total active power
2. $STot$ Total apparent power
3. $cos(\phi_1)$ Furnace power factor 1
4. $cos(\phi_2)$ Furnace power factor 2
5. $cos(\phi_3)$ Furnace power factor 3
6. V_1 electrode 1 to earth voltage (böckmann)
7. V_2 electrode 2 to earth voltage (böckmann)
8. V_3 electrode 3 to earth voltage (böckmann)

The selection of variables was determined through a process of trial and error. Reducing the quantity of inputs results in a reduction of the precision of the model. However, expanding the quantity of inputs does not necessarily result in a substantially more precise model. Rather, it elevates the model's order and, consequently, its complexity. Additionally, the model may exhibit overfitting of the data.

5 Model Selection

5.1 TRAINING, VALIDATION AND TEST DATASET

The dataset has been partitioned into three distinct subsets of data. Each individual subset comprises of a matrix consisting of the input values and another matrix representing the output values, which are referred to as targets.

The model is executed on a subset of the training data and subsequently evaluated against the target. The model is adjusted utilizing the System Identification toolbox in Matlab, according to the obtained results.

Subsequently, the model that has been fitted is used to predict the responses for the observations available in the subset of validation data. The purpose of this action is to avoid over-fitting to the subset of data used for training.

The test data subset is a subset that is utilized to offer an impartial assessment of a final model that has been fitted on the training data subset.

The complete dataset comprises a one-month duration, specifically from July 1st to August 1st, and has been sampled in the time-domain with a sample interval of one second. The time-domain data comprises the input and output variables of a system that are recorded at a consistent sampling interval throughout a specific time frame.

The dataset has been partitioned into three distinct subsets as delineated below:

- The last three days are used as test dataset
- 70% of the remaining is the training dataset

- the last 30% is the validation dataset

5.2 System Identification

The process of constructing mathematical models of dynamic systems through the utilization of input and output signal measurements is referred to as system identification.

In a dynamic system, the values of the output signals depend on both the instantaneous values of the input signals and also on the past behavior of the system. [12]

5.3 Black-box model

A black-box refers to a system that can be analyzed solely based on its inputs and outputs, without any understanding of its internal mechanisms. This approach can be beneficial when the main focus is on achieving a good fit for the data, without necessarily adhering to a specific mathematical structure of the model.

The selection of this methodology has been prioritized over a grey-box approach, which integrates qualitative prior knowledge with quantitative data. This decision is based on the lack of sufficient reliability in the prior knowledge pertaining to the SAF, making it inappropriate for constructing a conclusive model.

The process of black-box modeling typically involves a trial-and-error approach, wherein solely the response behavior is taken into consideration. Various parameters can be altered to obtain a model that fits well:

- type of model (ARX, ARMAX, BJ, OE)
- order of the model
- delay input/output

This study exclusively considers linear models as data-driven structure.

5.4 Model structures

4 distinct linear model structures have been considered.

- Arx
- Armax
- Output Error
- Box-Jenkins

5.4.1 Arx: Autoregressive with Extra Inputs

For this type of model, the noise is coupled with the dynamics of the system.

Given $u(t)$, $y(t)$ and $e(t)$ the input, the output and the error at time t, respectively:

$$A(q)y(t) = B(q)u(t - n_k) + e(t) \tag{5.1}$$

where

- q is the time shift/delay operator.
- n_k is the dead time, number of input samples that occur before the input affects the output.
- $A(q), B(q)$ matrices to estimate.

The limitation of this model is the lack of adequate freedom in describing the properties of the disturbance term $e(t)$ [12].

5.4.2 Armax: Autoregressive Moving Average with Extra Input

ARMAX extends the ARX model structure by incorporating the moving average (MA) of the noise signal in the model.

$$A(q)y(t) = B(q)u(t) + C(q)e(t) \tag{5.2}$$

where:

- C(q) is the estimated matrix associated with the error e(t).

5.4.3 OE: Output Error

OE models are useful when the disturbances can be modeled as white noise [12].

$$y(t) = \frac{B(q)}{F(q)}u(t) + e(t) \tag{5.3}$$

where:

- F(q) is the estimated matrix associated with the input u(t).

5.4.4 BJ: Box-Jenkins

BJ model is the most flexible model of those tested.

$$y(t) = \frac{B(q)}{F(q)}u(t) + \frac{C(q)}{D(q)}e(t) \tag{5.4}$$

where:

- D(q) is the estimated matrix associated with the error e(t).

5.5 Linear Armax Model

The best linear model found uses a third-order discrete-time ARMAX structure:

$$A(q)y(t) = B(q)u(t) + C(q)e(t) \tag{5.5}$$

where

- $A(q)$ is a 3-by-3 matrix.
- $B(q)$ is a 3-by-8 matrix.
- $C(q)$ is a 3-by-1 vector.

The model has no added delay between inputs and outputs.

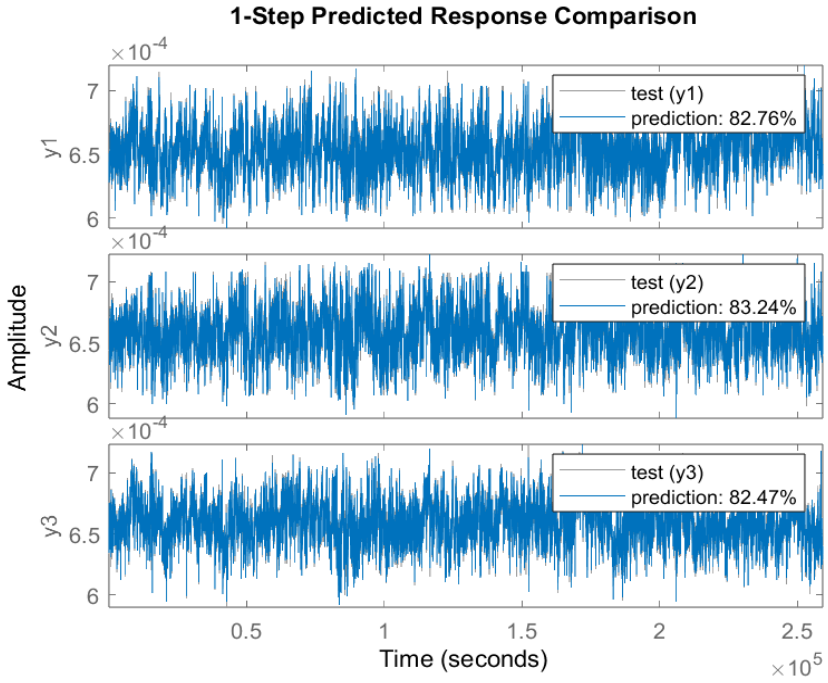

Figure 5.1: 1-step prediction on test dataset

The accuracy displayed in figure 5.1 is calculated as normalized root mean squared error (NRMSE).

$$accuracy = 100 * \left(1 - \frac{||y - \hat{y}||}{||y - mean(y)||}\right) \tag{5.6}$$

where y is the test data outputs and $\hat{y}$ is the output of model.

The efficacy of the model was evaluated by subjecting it to varying levels of total active power P, in smaller subsets of the data.

[Figure 5.2 shows the response of the model when the power P is lower than the average. In this case the average of the small portion is 46.08 MW while the average of the total measured data is 46.98 MW. The model seems to perform better with low active power for electrodes 1 and 2, while it's slightly worse for the third electrode.]

The graphical representation in figure 5.2 illustrates the model's reaction to a decrease in power P below the mean value. The current analysis reveals that the mean value of the minor subset is 46.08 MW, whereas the mean value of the entire set of observations is 46.98 MW. The model exhibits superior performance when the active power is low for electrodes 1 and 2, whereas it demonstrates a slightly inferior performance for the third electrode.

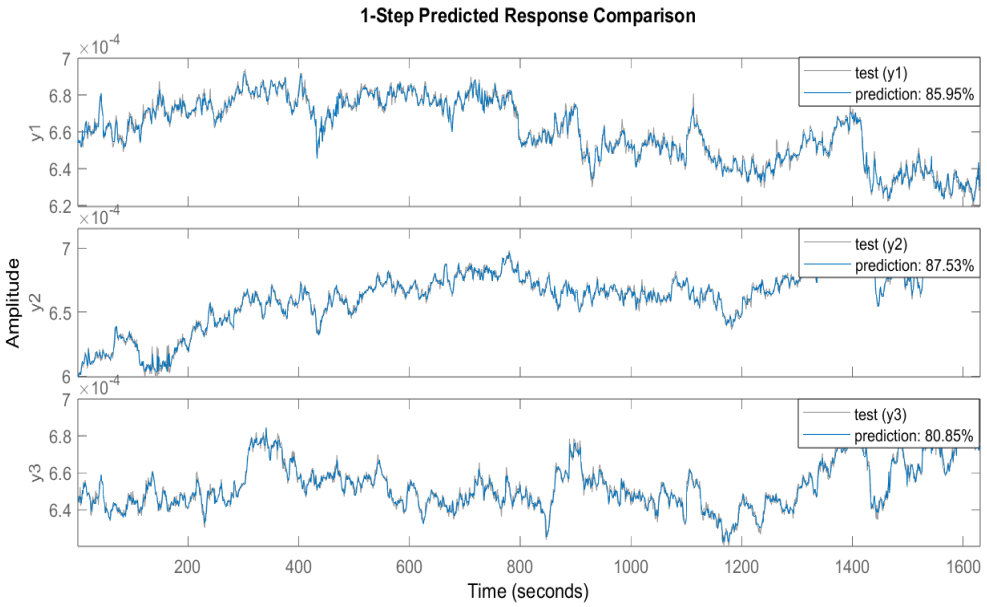

Figure 5.2: 1-step prediction with low total active power P

A similar result is shown in figure 5.3 where the total active power P is higher than the average with a mean of 47.91 MW.

Figure 5.3: 1-step prediction with high total active power P

5.6 Linear Box-Jenkins Model

When the BJ model is taken into consideration, a comparable outcome has been observed:

$$y(t) = \frac{B(q)}{F(q)}u(t) + \frac{C(q)}{D(q)}e(t) \tag{5.7}$$

where

- $B(q)$ is a 3-by-8 matrix.
- $C(q)$ is a 3-by-1 vector.
- $D(q)$ is a 3-by-1 matrix.
- $F(q)$ is a 3-by-8 matrix.

The model has no added delay between inputs and outputs.

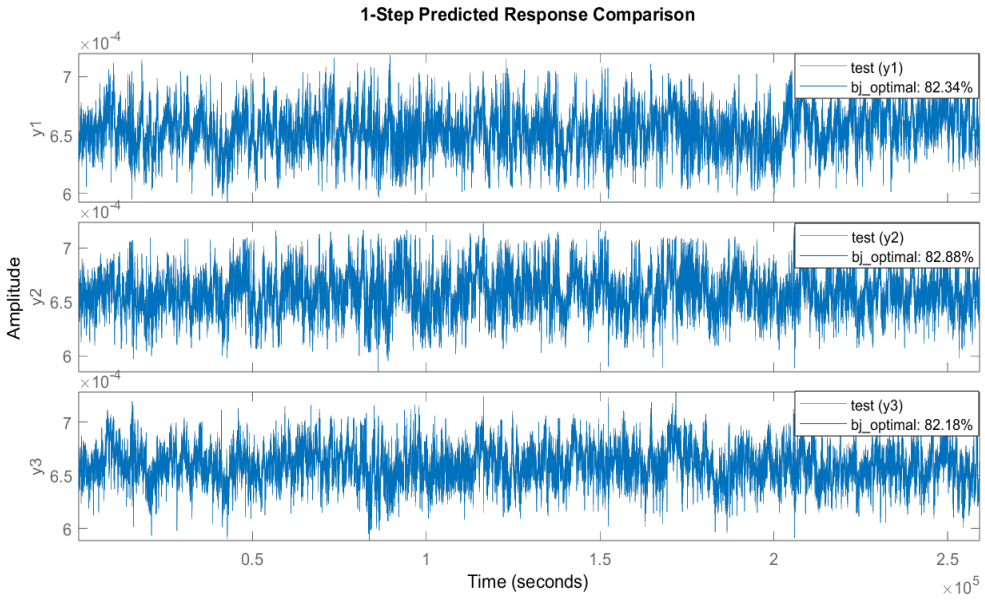

Figure 5.4: 1-step prediction on test dataset, BJ model

6 Metamodel

6.1 Definition of metamodel

Physics–based Finite Element Methods (FEM) models of submerged arc furnaces (SAF) can accurately estimate the induced currents in the steel shell, the alternating current distributions in the material layers, and the active and reactive power densities within the furnace. However, a physics-based model is generally very demanding in terms of computational time and resources, and therefore difficult to employ during control operations and in fast prototyping.

A metamodel is a data-driven surrogate of the original model that retains the same generalization capabilities as the original model while being computationally lightweight [13].

The metamodel is a linear model of the form:

$$y = \beta x \tag{6.1}$$

where y is an output vector of 126 elements and x is the internal state vector of 78 elements. The matrix β encompasses the coefficients that represent the affine mapping between the input and output variables. These coefficients are obtained through the application of a partial least squares regression (PLSR) approach.

The internal states are seen as the inputs of the meta-model and they are:

1. RMS Voltage at the transformer
2. Tip position of electrode 1

3. Tip position of electrode 2
4. Tip position of electrode 3
5. Crater wall thickness
6. Conductivity of crater wall 1
7. Conductivity of crater wall 2
8. Conductivity of crater wall 3
9. Sigma SiC 1-2
10. Sigma SiC 1-3
11. Sigma SiC 2-3
12. Elements 1-11 multiplied by each other
13. Elements 1-11 multiplied by themself

6.1.1 Tuning of the metamodel

The metamodel is a comprehensive representation of the furnace utilized by the industrial partners involved in the SAFECI project.

It may be necessary to calibrate the tuning of the measurement data to the particular Wacker furnace in question.

The raw data exclusively comprises characteristics that correspond to the output of the metamodel. This posed a challenge in accurately calibrating the simulator. An approach to achieving this objective involves determining the internal state values, denoted as x, that result in the minimal discrepancy between the outputs generated by the metamodel and the corresponding empirical observations.

$$\min_x |y - \hat{y}(x)| = \min_x |y - \beta x| \tag{6.2}$$

where y is the measured data and $\hat{y}$ is the output of the metamodel.

The measurement data provided for this project is insufficient to encompass the entire range of outputs produced by the metamodel.

It can be observed that the equation 6.2 possesses an infinite number of solutions.The problem can be resolved by constraining all internal states within a feasible range.

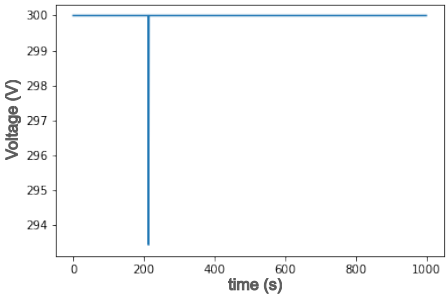

(a) Vms bounded in [250,300] V

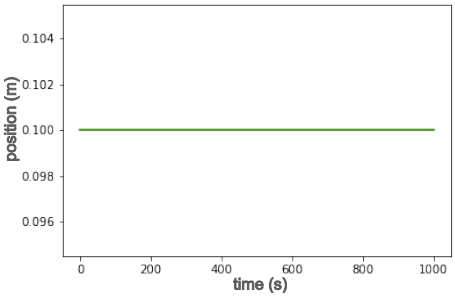

(b) Tip positions bounded in [0.1,0.75] m

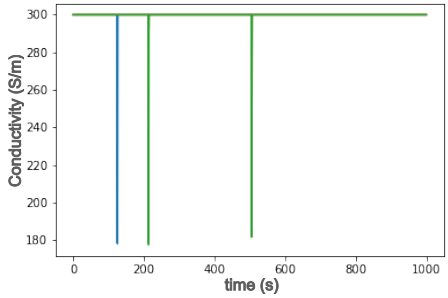

(c) Conductivity of crater wall [75,300] S/m

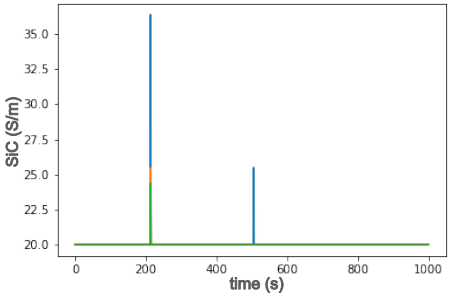

(d) SiC bounded in [20,75] S/m

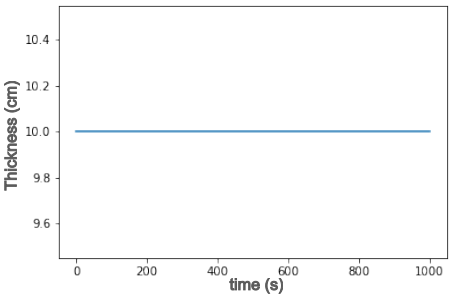

(e) Crater wall thickness bounded in [10,20] cm

Figure 6.1: Estimated internal states from equation (6.2)

According to Figure 6.1, it can be observed that the metamodel exhibits poor responsiveness towards the actual data values. In fact, all internal state values are estimated to be at their limits for a period of one thousand seconds. This solution is not feasible. This implies that the simulator must be calibrated to suit the particular furnace.

The time frame depicted in figure 6.2 is also illustrated in figure 6.1, although with an increased upper limit for voltage (figure 6.2a) and an absence of boundaries for crater wall thickness (figure 6.2e). Consequently, the feasibility of the internal states' value appears to be evident. The size of the Wacker's furnace exceeds that of the typical submerged arc furnace, thereby accounting for the elevated voltage levels observed.

The unfeasibility of figure 6.2e for an actual furnace is attributed to the presence of negative values. Given that all other variables are within the anticipated ranges, it is possible to draw the following potential conclusions:

- The metamodel is not accurate in the calculation of the crater wall thickness.
- The measurement data has too much noise to be reliable in calculation of the crater wall.

The accuracy of the internal states x, as provided by Equation (6.2), is compromised by the presence of intrinsic noise in the measurement data. The value of (6.2) is always non-zero and it exhibits convergence towards a certain value. The equation provides a preliminary indication of the feasibility of the metamodel.

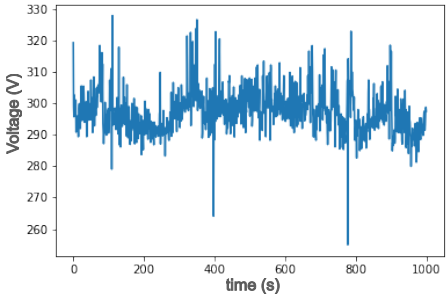

(a) Vms bounded in [250,400] V

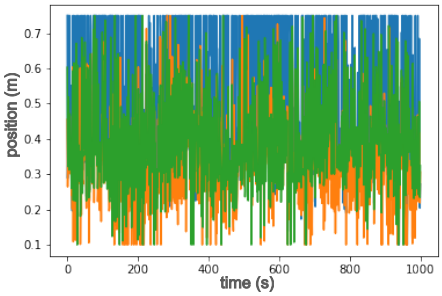

(b) Tip positions bounded in [0.1,0.75] m

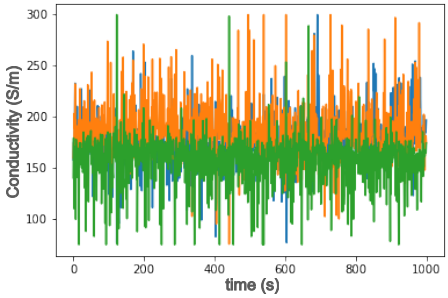

(c) Conductivity of crater wall [75,300] S/m

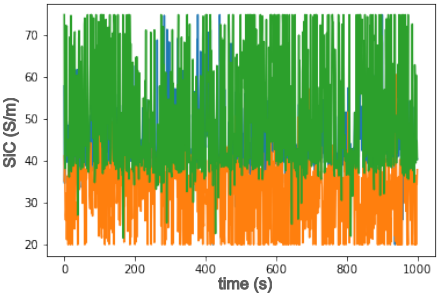

(d) SiC bounded in [20,75] S/m

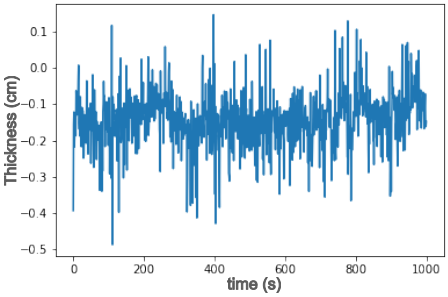

(e) Crater wall thickness bounded in [-inf,inf] cm

Figure 6.2: Relaxed estimated internal states from equation (6.2)

7 Comparison

7.1 Idea

One of the aims of this thesis is to undertake a comparison between the linear dynamic model and the static linear metamodel.

Initially, it is crucial to establish the inquiries that a comparison of two models attempts to address.

- Are the static of the two models similar under some metric?
- How well the static model captures the gain of the dynamic model?
- Do the dynamics give more information than the statics?
- Can the static simulator (metamodel) perform better with the information the dynamic model provides?

7.2 Challenges

The comparison is not straightforward. In fact, the metamodel lacks some of the states of the plant. The metamodel and the real measurements are fundamentally different organized:

- Simulator: All the measured signals are in the output and the internal states are in the input.
- Plant: Measured signals are both in the inputs and outputs

The inability of verification is attributed to the unknown nature of the internal states. The internal states might be constant in the plant (steady-state), but they are perceived as inputs by the metamodel.

There exists a mismatch between the inputs of the dynamic model and the internal states (inputs) of the metamodel. The absence of internal state in the measurement data dataset precludes a direct comparison of ”inputs to outputs” between the two models.

7.3 HOLDER POSITION VS TIP POSITION

There exists a known correlation between the holder position and the tip position, which can be mathematically expressed through the following formula:

$$Z = Z_0 + \Delta H + S - C \tag{7.1}$$

where:

- ΔH represents the vertical location of the electrode holder, which is subject to operator control. Its primary purpose is to regulate the resistance within the hot zone by enabling upward or downward movement. The measurement is provided by the dataset. The range of values spans from 20 to 140 centimeters.

- Z_0 represents the length of the electrode, and although its precise value is indeterminate, it is postulated to be always greater than to 50 centimeters.

- Z represents the position of the electrode tip. The metamodel's internal state is represented as a positive number within the interval of 100 to 750 centimeters.

- S denotes the phenomenon of slipping. The phenomenon occurs periodically, with a frequency of hours, and serves to regenerate the electrode that has been depleted during the process.

- C is the natural consumption of the electrode.

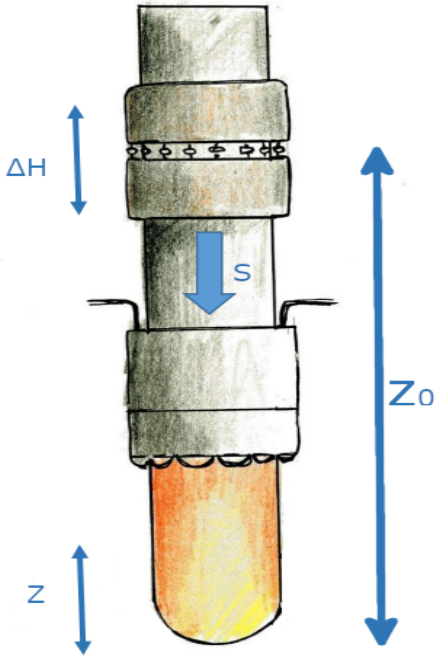

Figure 7.1: Electrode representation

Figure 7.2 depicts a theoretical illustration of the electrode's tip position. The vertical displacement of the tip is a result of the electrode's self-consumption over time. The electrode is reconstructed by the slipping process at a specific time T, in the order of hours. The slipping rate is subject to the discretion of the operators.

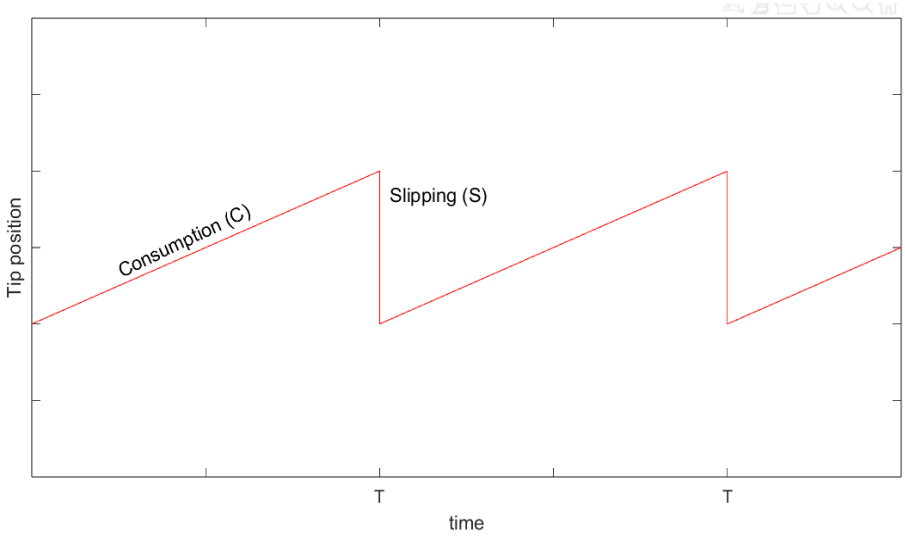

Figure 7.2: Electrode consumption over time

Assuming that S and C cancel themself out (especially in small time intervals), is it possible to estimate the length of the electrode Z_0? In other words, can a linear regression model describe the relation between Z, Z_0, and ΔH through the following formula?

$$Z = Z_0 + \Delta H \tag{7.2}$$

If such is the case, there exists a direct correlation between a potential input of the dynamic model and an internal state of the metamodel.

The equation 6.2 was utilized to establish a temporal correlation between the holder position ΔH and the tip position Z, thereby enabling the recreation of the value of the tip position within a specific time interval. A linear regression has been constructed using the two variables:

$$Z = Z_0 + x\Delta H \tag{7.3}$$

where Z_0 is the intercept that has been estimated.

The coefficient of determination R^2 has been calculated in order to evaluate how well the model fit the data. The result is $R^2 = 0.0022$, where the best possible score is 1.0. Hence the linear regression model doesn't fit the data as expected. Therefore, it is not acceptable to assume the equation 7.2 as being reliable. As a result, the data regarding the holder's positions is being excluded from the dataset of the dynamic model.

7.4 STEADY-STATE VS METAMODEL

As stated in Section 7.3, there exists no direct correlation between the inputs of the dynamic model and the internal states of the metamodel.

Thus, an approach has been pursued to compare the inputs of the dynamic model with the outputs of the metamodel.

The proposed approach involves partitioning the results of the linear equation of the metamodel into components that serve as inputs and outputs for the dynamic model, as well as extraneous values that are not utilized by the dynamic model.

$$\boldsymbol{y_m} = \begin{bmatrix} y_d \\ u_d \\ z_d \end{bmatrix} = \begin{bmatrix} \beta_1 \\ \beta_2 \\ \beta_3 \end{bmatrix} \boldsymbol{x_m} = \boldsymbol{\beta x_m} \tag{7.4}$$

Where y_d and u_d are the outputs and the inputs, respectively, of the dynamic model in steady-state form.

The steady-state form is given by the state-space representation of the dynamic model:

$$x_{d+1} = Ax_d + Bu_d \tag{7.5}$$

$$y_d = Cx_d + Du_d \tag{7.6}$$

where x_{d+1} and x_d are assumed to be equal so that:

$$(I - A)\, x_d = Bu_d \tag{7.7}$$

and so:

$$y_d = \underbrace{\left(C(I - A)^{-1}B + D\right)}_{K} u_d \tag{7.8}$$

Inserting (7.5) into (7.8), it becomes:

$$\underbrace{\beta_1 x_m}_{y_d} = \left(C(I - A)^{-1}B + D\right) \underbrace{\beta_2 x_m}_{u_d} \tag{7.9}$$

and it can be re-written as:

$$\underbrace{\left(\beta_1 - \left(C(I - A)^{-1}B + D\right)\beta_2\right)}_{M} x_m = 0 \tag{7.10}$$

Matrix M contains uncertainties derived by matrix K of equation (7.8).

Solving matrix M gives a suggestion of what the internal states are for the dynamic model.

M is a 3-by-78 matrix (not square!). This implies that the kernel of M has infinite solutions.

The imposition of certain boundaries on the internal states of matrix M serves to decrease the quantity of feasible solutions. Nonetheless, this approach faces

analogous challenges as explicated in section 6.1.1. The reliability of defining precise boundaries is compromised by the inadequacy of metamodel tuning.

This approach may prove to be efficacious if one or more internal state variables are measurable.

7.5 DYNAMIC MODEL VS LINEAR REGRESSION

In order to assess the efficacy of the applied methodology in model creation, a comparative analysis was conducted between the subject model and a model developed using linear regression.

Linear regression is a statistical technique that aims to establish a mathematical relationship between two variables by employing a linear equation to best fit the observed data. One variable is designated as the independent variable (inputs of the model), while the other is designated as the dependent variable (outputs of the model). The objective of linear regression is to minimise the residual sum of squares between the observed targets in the dataset and the targets predicted by the linear approximation.

$$y = A + Wu \tag{7.11}$$

Where

- y and u are the same ouputs and inputs of the dynamic model.
- A is the intercept matrix.
- W is the coefficients matrix.

Once the estimation of matrix A and W in equation (7.11) has been performed using the training dataset, the model is eventually analysed against the dynamic model in the validation dataset.

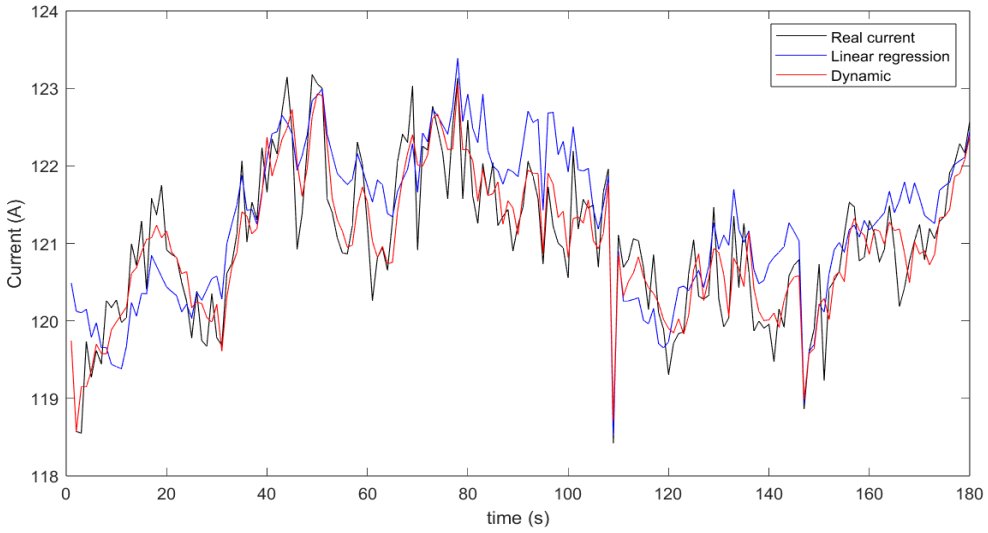

Figure 7.3: Current: real value (black), linear regression (blue), dynamic model (red)

Despite the adequate fit of the linear regression model to the data, its accuracy remains inferior to that of the dynamic model. Indeed, the accuracy of the two models and the actual output current can be assessed based on their goodness of fit:

	Current 1	**Current 2**	**Current 3**
Dynamic model	96.95%	97.57%	97.09%
Linear regression model	90.81%	92.09%	89.95%

7.6 DYNAMIC MODEL VS STEADY-STATE

In Section 7.4, the model has been assumed to be in a steady-state condition for the purpose of comparison. This section presents an analysis of the dynamic model to determine whether the assumption of steady-state can be made for the plant, taking into consideration the system's slow dynamics. The steady-state model described in equation (7.8) is compared with the dynamic model.

The output currents are compared to the actual current value for a given input:

	Current 1	**Current 2**	**Current 3**
Dynamic model	96.95%	97.57%	97.09%
Steady-state	84.38%	85.68%	82.51%

The steady-state model appears to exhibit inferior performance compared to the dynamic model, although the trade-off between reduced accuracy and increased simplicity may be considered acceptable.

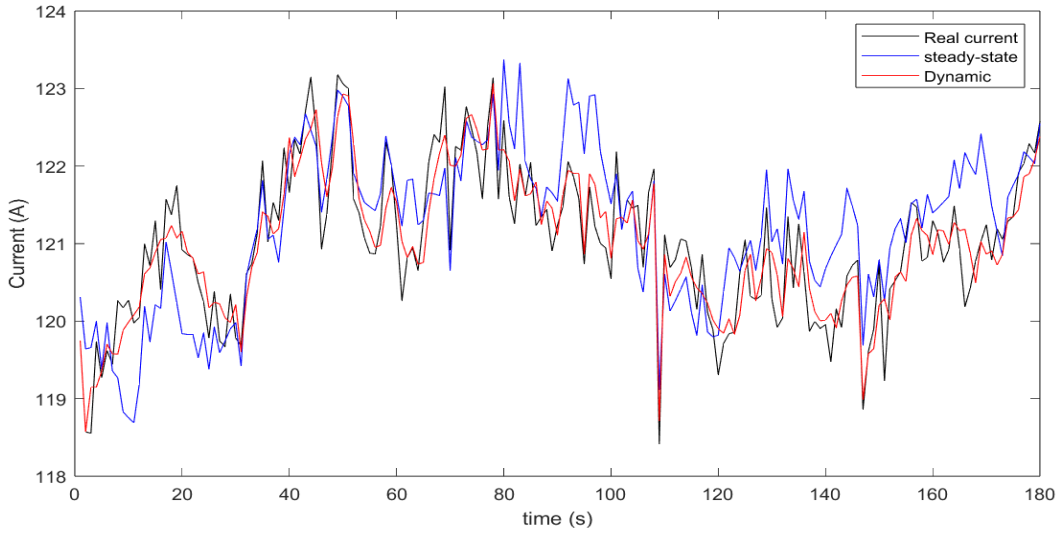

Figure 7.4: Current: real value (black), steady-state (blue), dynamic model (red)

8

Conclusions and Future Works

The goal of this study was to determine the optimal linear data-driven model for submerged arc furnaces. This paper elucidates various methodologies employed in attempting to compare a model with an existing meta-model, while also providing an explanation as to why such a comparison is unattainable.

Ultimately, the model has been demonstrated to outperform a linear regression model.

A portion of the research conducted in this project has been incorporated into a forthcoming publication *"Data Driven System Identification for the Modelling of Submerged Arc Furnaces"*. The paper examines both linear and non-linear models, providing analysis for both cases.

Following works related to this project will involve improving the step prediction capabilities of the models, specifically by extending the prediction horizon to include intervals as short as 5 minutes.

A Appendix

A.1 Measurement dataset

Parameters	Definition	Formula
$I_1(A)$	rms current for electrode 1	
$I_2(A)$	rms current for electrode 2	
$I_3(A)$	rms current for electrode 3	
$GI_1(m)$	Holder position of the electrode 1	
$GI_2(m)$	Holder position of the electrode 2	
$GI_3(m)$	Holder position of the electrode 3	
$V_1(V)$	electrode 1 to earth voltage (Böckmann)	
$V_2(V)$	electrode 2 to earth voltage (Böckmann)	
$V_3(V)$	electrode 3 to earth voltage (Böckmann)	
$P(MW)$	Total Active Power	
$QTot$	Total Reactive Power	
$STot$	Total Apparent Power	$STot = \sqrt{P^2 + QTot^2}$
$cos(\phi_1)$	Furnace Power Factor 1	
$cos(\phi_2)$	Furnace Power Factor 2	
$cos(\phi_3)$	Furnace Power Factor 3	
$ElCos(\phi_1)$	Electrode Power Factor 1	Directly from the meter
$ElCos(\phi_2)$	Electrode Power Factor 2	Directly from the meter
$ElCos(\phi_3)$	Electrode Power Factor 3	Directly from the meter
P_1	Power of electrode 1	$P_1 = V_1 * I_1 * ElCos(\phi_1)$

P_2	Power of electrode 3	$P_3 = V_2 * I_2 * ElCos(\phi_3)$
P_3	Power of electrode 3	$P_3 = V_3 * I_3 * ElCos(\phi_3)$
$CalcResTot(m\Omega)$	Total resistance of the furnace	$R = \frac{3*Effekt}{(I_1+I_2+I_3)}$
$R_1(m\Omega)$	Resistance of electrode 1	$R_1 = P_1/(I_1)^2$
$R_2(m\Omega)$	Resistance of electrode 2	$R_2 = P_2/(I_2)^2$
$R_3(m\Omega)$	Resistance of electrode 3	$R_3 = P_3/(I_3)^2$
X_1	Reactance of electrode 1	$X_1 = V_1 * \sqrt{\frac{(1-ElCos(\phi_1)}{I_1}}$
X_2	Reactance of electrode 2	$X_2 = V_2 * \sqrt{\frac{(1-ElCos(\phi_2)}{I_2}}$
X_3	Reactance of electrode 3	$X_3 = V_3 * \sqrt{\frac{(1-ElCos(\phi_3)}{I_3}}$
$FurnaceC3$		$C3 = \frac{1}{3} * \frac{(I_1+I_2+I_3)}{\sqrt[3]{Effekt^2}}$
QI	Crucible thermal flux	
GI	Crucible rotational position	

References

[1] Aasgeir Mikael Valderhaug. "Modelling and control of submerged-arc ferrosilicon furnaces." In: (1995).

[2] Emma Cuthbert et al. *Data Driven System Identification for the Modelling of Submerged Arc Furnaces*. 2023.

[3] Thorsteinn Hannesson. *The SI process - DRAWINGS*. 2016.

[4] Jesse F White et al. "Thermal properties of Söderberg electrode materials". In: *Metallurgical and Materials Transactions B* 51 (2020), pp. 1928–1932.

[5] Kristian Stråbø. "Report – Visiting the plant in Sauda". Report.

[6] IJ Barker et al. "The interaction effect in submerged-arc furnaces". In: *Electric Furnace Conference Proceedings.* Vol. 49. 1991, pp. 305–310.

[7] B Asphaug. *FeMn Production*. 1997.

[8] Stef Van Buuren and Karin Groothuis-Oudshoorn. "mice: Multivariate imputation by chained equations in R". In: *Journal of statistical software* 45 (2011), pp. 1–67.

[9] Samuel F Buck. "A method of estimation of missing values in multivariate data suitable for use with an electronic computer". In: *Journal of the Royal Statistical Society: Series B (Methodological)* 22.2 (1960), pp. 302–306.

[10] Melissa J Azur et al. "Multiple imputation by chained equations: what is it and how does it work?" In: *International journal of methods in psychiatric research* 20.1 (2011), pp. 40–49.

[11] Robert Tibshirani. "Regression shrinkage and selection via the lasso". In: *Journal of the Royal Statistical Society: Series B (Methodological)* 58.1 (1996), pp. 267–288.

[12] Lennart Ljung et al. "Theory for the user". In: *System identification* (1987).

[13] Manuel Sparta et al. “Metamodeling of the electrical conditions in submerged arc furnaces”. In: *Metallurgical and Materials Transactions B* 52 (2021), pp. 1267–1278.

Acknowledgments

I would want to express my gratitude to Damiano, my supervisor, for providing me with the opportunity to work with such an exceptional team. Without his assistance, I would not have been able to embark on this path.

The accomplishment of this thesis would not have been possible without Hans, Håvard and Emma's assistance and the knowledge they passed on to me.

I owe an enormous debt of gratitude to my supervisors at Norce, Manuel and Vetle for providing me with the chance to work for a company as remarkable as Norce and for making themselves available to me at any time I required assistance or clarification.

Vorrei ringraziare di cuore i miei cari genitori per il loro costante sostegno e incoraggiamento nel perseguire nuove esperienze. Senza di voi, non avrei mai avuto l'opportunità di entrare in contatto con culture diverse e di stringere legami preziosi con persone che ora considero cari amici. Il vostro supporto è stato fondamentale per arricchire il mio percorso e ampliare le mie prospettive.

I'm also grateful to my Swedish family for allowing me to witness for the first time what I believed was only possible in movies: the formation of such a strong friendship that extends long beyond the Erasmus program. I hope it will continue indefinitely, despite the constraints of our hectic lives.

Special thanks to all the friends that I made in Norway. It's true that expat life may be rewarding, but only if you surround yourself with people who share your enthusiasm for exploring the world.

Finally, I'd like to thank all of the friends I've made over the years. You are the reason I'm happy to come back to Italy. I hope that no matter what I'm gonna do work-wise, we'll be able to meet and catch up from time to time.